Ferroelectricity induced by oxygen vacancies in relaxors with perovskite structure

Maya D. Glinchuk,[1] Eugene A. Eliseev,[1] Guorong Li,[2] Jiangtao Zeng,[2] Sergei V. Kalinin,[3] and Anna N. Morozovska[4,*]

[1]*Institute for Problems of Materials Science, National Academy of Sciences of Ukraine, Krjijanovskogo 3, 03142 Kyiv, Ukraine*

[2]*Key Laboratory of Inorganic Functional Material and Device, Shanghai Institute of Ceramics, Chinese Academy of Sciences, 1295 Dingxi Road, Shanghai 200050, China*

[3]*The Center for Nanophase Materials Sciences, Oak Ridge National Laboratory, Oak Ridge, Tennessee 37831, USA*

[4]*Institute of Physics, National Academy of Sciences of Ukraine, 46, pr. Nauky, 03028 Kyiv, Ukraine*

(Received 31 March 2018; revised manuscript received 18 June 2018; published 4 September 2018)

The influence of oxygen vacancies on the relaxors with perovskite structure was considered in the framework of Landau-Ginzburg-Devonshire phenomenological theory. We focused on the PZN-PLZT relaxor, where an earlier experimental investigation of the influence of oxygen vacancies on the polar properties was performed and evidence of oxygen vacancy induced ferroelectricity was obtained. Since the oxygen vacancies are known to be elastic dipoles, they affect the elastic and electric fields due to Vegard and flexoelectric couplings. We have shown that a negative Curie temperature $T_C{}^*$ of a relaxor is renormalized by the elastic dipoles due to the electrostriction coupling and could become positive at some large enough concentration of the vacancies. A positive renormalized temperature $T_C^R = T_C^* + \Delta T$ is characteristic for the ferroelectric state. At $T < T_C^R$, all the polar properties could be calculated in the conventional way for ferroelectrics, but the obtained experimental data favor the coexistence of the ferroelectric phase with a relaxor state, i.e., the presence of a morphotropic region in PZN-PLZT relaxor. At $T > T_C^R$, the random field characteristic for relaxors is preserved, but since the mean square deviation of the polarization is nonzero, the coexistence with a dipole glass state is not excluded. For the case $T > T_C^R$, we calculated the local polarization and electric field induced by the flexochemical coupling with oxygen vacancies.

DOI: 10.1103/PhysRevB.98.094102

I. INTRODUCTION

The broad application of relaxor ferroelectrics in modern sensors, actuators, high performance electromechanical transducers, and other electronic devices [1,2] constantly generates interest in the investigation and fabrication of these materials. These applications are based on the peculiar properties of the relaxors absent in ordinary ferroelectrics [3]. The peculiarities appear due to random electric fields induced by two factors. The first one is substitutional disorder in cation positions because the general formula can be written as $A_{1-x}A'_xB_{1-y}B'_yO_3$, which leads to a local shift of ions from their conventional equilibrium positions. The second one is the presence of vacancies and other unavoidable defects. In previous years the influence of random fields was considered in great detail (see, e.g., references in Ref. [3] with special attention to Refs. [4,5]), but the attention was concentrated mainly on the first factor, which is inherent to any relaxor. The changes of oxygen vacancies concentration (V_O) can open a way to manipulate the relaxor properties, which motivates us to study the influence of V_O on properties. To the best of our knowledge, V_O were considered theoretically mainly as random field sources up to now. As for experimental papers on this topic, we would like to draw your attention to Ref. [6], where the influence of V_O on the phase diagram and properties were studied. The authors considered the PZN-PLZT relaxor. They increased the V_O concentration by addition of nitrogen flow when sintering the relaxor (NS samples), and after this procedure some of the samples were annealed in oxygen (OA samples). Comparative analysis of the dielectric permittivity temperature dependence of NS and OA samples showed that the relaxor characteristics were suppressed by inducing oxygen vacancies with high concentration. In other words, V_O added a ferroelectric (FE) phase to the relaxor. The aim of this paper is to find out the physical mechanism of FE phase induced by V_O.

II. OXYGEN VACANCIES IN THE RELAXORS AND THEIR CHARACTERISTIC FEATURES

Oxygen vacancies in ABO_3 ferroelectrics greatly impact their physical properties (see Ref. [6] and references therein) and the perovskite structure is able to conserve the structure stability even for high concentration of oxygen vacancies [7]. B cations are usually shifted from the central position in the neighborhood of an oxygen vacancy, because in ABO_3 structure the size of oxygen ions and their vacancies is larger than the size of the cations and their vacancies. To compensate for the loss of oxygen negative charges, the equivalent amount of B^{4+} cations should be in a B^{3+} state. The PZN-PLZT samples sintered in nitrogen atmosphere appeared to be black and opaque [6] because off-central Ti^{4+} transforms into color center Ti^{3+}. Note that Ti^{3+} can create layers of ordered dipoles at large concentration of oxygen vacancies [8]. The electrons necessary for the transformation of Ti^{4+} into Ti^{3+} can be

*Corresponding author: anna.n.morozovska@gmail.com

created from the ionization of neutral oxygen vacancy $V_O \rightarrow V_O^{\bullet} + e$, $V_O^{\bullet} \rightarrow V_O^{\bullet\bullet} + e$, the $V_O^{\bullet}$ and $V_O^{\bullet\bullet}$ being positively charged vacancies. The uncharged vacancy V_O represents a dilatational center, which creates local compressive strain.

Since generally the conductivity is mainly attributed to the electromigration of oxygen vacancies (see Refs. [9,10]) in perovskite ferroelectrics, measurements of *dc* conductivity temperature dependence of the NS and OA specimens were carried out in order to estimate the oxygen vacancy concentration and charge states. It was shown that NS specimens have several orders larger conductivity at high temperature (>300 °C). A comparison of activation energies extracted from the conductivity temperature dependence showed that the concentration of oxygen vacancies in the NS samples is high and attributed to $V_O^{\bullet\bullet}$ at low temperatures, while in OA samples contributions of $V_O^{\bullet\bullet}$ and $V_O^{\bullet}$ were detected at high and low temperatures, respectively. As to the high-temperature activation energy in NS specimens (0.95 eV), which appeared to be smaller than that in OA specimens (1.54 eV), the authors of Ref. [6] wrote that this effect is attributed to the higher concentration of oxygen vacancies in NS samples. To our mind, this statement could be correct for the same type of vacancies in both samples, e.g., compare E_a for $V_O^{\bullet\bullet}$ in them. A singly ionized vacancy with $E_a =$ 0.95 eV has also to be rejected because for such vacancy in an AO sample, $E_a = 0.31$ eV, which is much smaller than the 0.95 eV energy in the NS sample with a much larger concentration of oxygen vacancies. Because of this, we suggest that uncharged vacancies can contribute, as we will show later, to the activation energy of 0.95 eV in NS samples when complete compensation of loss oxygen negative charge 2e originates from two off-central Ti^{3+} ions. Because this complex defect can be represented as $V_O^{\bullet\bullet} + 2Ti^{3+}$, it can be observed in the high-temperature region only. Therefore, in the NS sample with the high concentration of oxygen vacancies, we see evidence of existence of $V_O^{\bullet\bullet}$ and V_O.

Note that vacancies tend to accumulate in the vicinity of any inhomogeneities, surfaces, and interfaces, since the energy of vacancy formation in such places can be much smaller than in the homogeneous volume [11–14]. In the places of vacancy accumulation they can create sufficiently strong fields, which in turn can lead to the appearance of new phases in relaxors, for example, polar (ferroelectric) phases. On the contrary, in places where there are few vacancies, the nonpolar relaxor remains. So, a coexistence of polar ferroelectric and nonpolar relaxor states can be realized in the case.

III. TEMPERATURE DEPENDENCE OF MODIFIED DIELECTRIC PERMITTIVITY IN PZN-PLZT NS SPECIMEN

It is well-known (see, e.g., Ref. [15]) that the temperature dependence of the dielectric permittivity of a ferroelectric relaxor can be described by a modified Curie-Weiss law:

$$\frac{1}{\varepsilon} - \frac{1}{\varepsilon_{\max}} = \frac{1}{K}(T - T_M)^p. \quad (1)$$

Here, $p = 2$, T_M marks the temperature of the dielectric permittivity maximum, K is a constant, while for normal ferroelectrics $T_M = T_C$, $p = 1$, and T_C is the Curie temperature. This difference originates from the relaxor's broken translational symmetry, so the modified Curie-Weiss law includes the frequency dependence in ε and also in T_M contrary to the classical Curie-Weiss law for ferroelectrics. The pronounced frequency dependence in relaxors is known to be produced by the broad relaxation time spectrum, described by the Vogel-Fulcher law $1/\tau = (1/\tau_0)\exp[-U/(k(T-T_g))]$, where T_g is the freezing temperature. This and other peculiarities of relaxor ferroelectrics originate from random electric field, induced by substitutional disorder, presence of vacancies, and other unavoidable defects (see, e.g., Ref. [3] and references therein).

Deng *et al.* [6] measured the temperature dependence of PZN-PLZT relaxor dielectric permittivity for NS and AO samples and obtained respectively $p = 1.53$ and 1.91. The obtained data speaks in favor of the statement that large concentration of oxygen vacancies induces ferroelectricity in the NS sample, which coexists with the relaxor state. This compound looks like $PMN_{1-x}PT_x$ solid solution, where one could observe the so-called morphotrophic region where relaxor and polar phases coexist (see, e.g., Ref. [16]). In what follows, we will consider the physical mechanism of induced ferroelectricity.

IV. POSSIBLE MECHANISMS OF FERROELECTRICITY INDUCED BY OXYGEN VACANCIES

Let us briefly consider possible mechanisms of ferroelectricity in NS samples of PZN-PLZT. As we discussed above, the oxygen vacancies in this sample are uncharged V_O, and singly and doubly positively charged $V_O^{\bullet}$ and $V_O^{\bullet\bullet}$, respectively. Because of the required oxygen loss, negative charges compensating approximately an equivalent amount of Ti^{3+} off-central ions is another group of defects. Keeping in mind the electrostriction in disordered systems the elastic dipoles transform into electric ones.

An illustration of the oxygen vacancy related defect configurations in a tetragonal perovskite lattice structure is shown in Fig. S1 in Ref. [17], adapted from Ref. [18]. The existence of electric dipoles will lead to the appearance of a ferroelectric phase due to the indirect interaction of dipoles via soft optic modes [19]; the soft mode existence in the ferroelectric relaxors will be discussed later.

Allowing for that, all the electric dipoles in the regions with sizes of order of correlation radius r_c must be oriented, and one can write the criterion of ferroelectric phase appearance as $Nr_c^3 \geqslant 1$, where N is the concentration of dipoles. In what follows we will name the lowest concentration $N_c = r_c^{-3}$ the correlation threshold.

Another possible mechanism of ferroelectricity in the relaxors can originate from an inhomogeneous elastic field via the flexoelectric effect, namely, $P_i = f_{ijkl}\partial u_{kj}/\partial x_l$, where P_i is the electric polarization component, $\partial u_{ij}/\partial x_l$ is the mechanical strain gradient, and f_{ijkl} is the tensor components of the flexoelectric effect. Detailed consideration of this mechanism along with the mechanical strain field originating from oxygen vacancies (Vegard mechanism) will be performed in the next part.

V. VEGARD STRAINS CONTRIBUTION TO APPEARANCE OF FERROELECTRICITY IN RELAXORS

Gehring *et al.* [20] performed neutron inelastic scattering measurements of the lowest-energy transverse optic (TO) phonon branch in the relaxor $Pb(Mg_{1/3}Nb_{2/3})O_3$ from 400 to 1100 K. Far above the Burns temperature $T_d = 620$ K, Gehring *et al.* observed well-defined propagating TO modes at all wave vectors q, and a zone center TO mode that softens in a manner consistent with that of a ferroelectric soft mode. Below T_d, the zone center TO mode is overdamped and its direct measurement becomes cumbersome. However, Gehring *et al.* [21] supposed that this mode recovers as has been reported for PZN, where at 20 K a TO mode was observed. The latter is very important for us because it was considered in Ref. [6] in the PZN-PLZT relaxor described by the formula $0.3Pb(Zn_{1/3}Nb_{2/3})O_3-0.7(Pb_{0.96}La_{0.04}(Zr_xTi_{1-x})_{0.99}O_3)$ with the composition ($x = 0.52$) near the morphotropic phase boundary, where the La concentration is 4% and so it has no relaxor properties, so that relaxor type behavior has to originate mainly from PZN. Therefore we came to the possibility of introducing a hidden soft mode in the considered relaxor. This permits us to use an LGD-type free energy functional for the quantitative consideration of ferroelectricity induced by oxygen vacancies in the relaxors. Note that the same approach was used earlier in Ref. [22] for the description of the relaxor ferroelectric PLZT ceramics with 8% and 9% of La and PZN–4.5%PT single crystals.

Note that the applicability of the standard Landau phenomenological model for calculation of the electrocaloric effect in relaxor ferroelectrics in Ref. [23] is out of doubt because of the induced by the electric field polarization. The Gibbs potential density of a relaxor ferroelectric material having some hidden soft phonon polar mode [20,21,24] has the following form [25]:

$$\begin{aligned} G = {} & \frac{\alpha(T)}{2}P_iP_j + \frac{\alpha_{ijkl}}{2}P_iP_jP_kP_l + \frac{g_{ijkl}}{2}\frac{\partial P_i}{\partial x_j}\frac{\partial P_k}{\partial x_l} \\ & + \frac{F_{ijkl}}{2}\left(\sigma_{kl}\frac{\partial P_i}{\partial x_j} - P_i\frac{\partial \sigma_{kl}}{\partial x_j}\right) - Q_{ijkl}\sigma_{ij}P_kP_l \\ & - \frac{s_{ijkl}}{2}\sigma_{ij}\sigma_{kl} + k_BT\ S(N_d, N_d^+) \\ & - P_iE_i - W_{ij}N_d(\vec{r})\sigma_{ij}, \end{aligned} \tag{2}$$

where P_i are the components of polarization vector ($i = 1$, 2, 3) and σ_{ij} is the elastic stress tensor. The summation is performed over all repeated indices. The dielectric stiffness coefficient $\alpha(T)$ is positive because the intrinsic ferroelectricity is absent, but depends on temperature reflecting the fact that the hidden phonon mode could soften at negative absolute temperatures. This statement follows from the abovementioned fact that in the PZN a soft mode was observed at $T = 20$ K, so that its frequency could be zero at negative temperature. Note that extrapolation of the PMN soft mode frequency to zero leads to $T_c \approx -150$ K. The matrix of the gradient coefficients g_{ijkl} is positively defined. Q_{ijkl} is the electrostriction tensor, s_{ijkl} is the elastic compliances tensor, and F_{ijkl} is the forth-rank tensor of flexoelectric coupling. Note that a detailed consideration of the coupling contribution will be performed in the next section. The configuration entropy function $S(x, y)$ is taken as $S(x, y) = y\ln(y/x) - y$ in the Boltzmann-Planck-Nernst approximation, $k_B = 1.3807 \times 10^{-23}$ J/K, where T is the absolute temperature.

In Eq. (2), $E_i(\mathbf{r})$ denotes the internal electric field that satisfies the electrostatic equation

$$\varepsilon_b\varepsilon_0\frac{\partial E_i}{\partial x_i} + \frac{\partial P_i}{\partial x_i} = e(N_d^+ - n), \tag{3}$$

where ε_b is the background permittivity [26] and $\varepsilon_0 = 8.85 \times 10^{-12}$ F/m is the universal dielectric constant, $e(N_d^+ - n)$ is the space charge density of singly ionized vacancies and electrons, and $e = 1.6 \times 10^{-19}$ C is an electron charge. The field $E_i(\mathbf{r})$ is induced by nonzero divergence of the bound charge $\frac{\partial P_i}{\partial x_i}$ (depolarization contribution) and space charge fluctuations related to ionized vacancies (random field contribution).

Taking into account that the "net" random electric fields should be created by charged defects [4,27], they are not the local fields originating around randomly distributed elastic dipoles due flexoelectric effect, but rather quenched by Imry-Ma scenario random fields [28]. It should be argued that the amount of charged vacancies is usually much smaller than the amount of uncharged vacancies, which are considered below as the main sources of ferroelectricity allowing for the Vegard mechanism. Actually, as a rule, the concentration of the charged defects (ionized vacancies in our case) is of the order of several percents of the total defect concentration in the volume of the material, with the exception of near-surface charged layers, where their accumulation or depletion is possible [29]. The maximum number of vacancies observed in NS samples in Ref. [6] is related to uncharged oxygen vacancies (i.e., to elastic dipoles).

The equations of state $\partial G/\partial\sigma_{ij} = -u_{ij}$ determine the strains u_{ij}. The Euler-Lagrange equations $\partial G/\partial P_i = 0$ determine the polarization components. The last term in Eq. (2) is the *Vegard-type* concentration-deformation energy, $W_{ij}N_d\sigma_{ij}$, determined by the elastic defects (e.g., charged or electroneutral oxygen vacancies) with fluctuating concentration $N_d(\mathbf{r}) \cong \langle\sum_k \delta(\mathbf{r} - \mathbf{r}_k)\rangle \equiv \bar{N}_d + \delta N_d(\mathbf{r})$, where the equilibrium concentration is $\bar{N}_d$, and $\delta N_d(\mathbf{r})$ is the random variation. The variation $\delta N_d(\mathbf{r})$ is characterized by zero spatial average and nonzero mean square dispersion values, i.e., $\langle\delta N_d(\mathbf{r})\rangle = 0$ and $\langle\delta N_d^2(\mathbf{r})\rangle = n_d^2 > 0$. Different cases, $\bar{N}_d \gg n_d$, $\bar{N}_d \sim n_d$, and $\bar{N}_d \ll n_d$, are possible for oxygen vacancies. The average distance between defects centers $2R$ should be associated with the *average volume per inclusion* and so is defined from the relation $\frac{4\pi}{3}R^3 = \frac{1}{\bar{N}_d}$. The defect size r_0 is much smaller than the average distance R, e.g., r_0 is the ionic radius $\sim(0.1-1)$Å^3 (see Fig. 1).

The nonzero components of the Vegard stresses induced by a spherically symmetric elastic point defect (e.g., dilatation centre) located in the coordinate origin, $\mathbf{r} = 0$, in spherical coordinates have the form [30]

$$\begin{aligned} \sigma_{rr}^W(\mathbf{r}) &= \frac{-W_{rr}}{2\pi(s_{11} - s_{12})r^3}, \\ \sigma_{\theta\theta}^W(\mathbf{r}) &= \sigma_{\varphi\varphi}^W(\mathbf{r}) = \frac{W_{\theta\theta}}{4\pi(s_{11} - s_{12})r^3}. \end{aligned} \tag{4}$$

Equations (4) are derived under the assumption of isotropic and diagonal Vegard expansion tensor W_{ij}, $W_{ij} = W\delta_{ij}$.

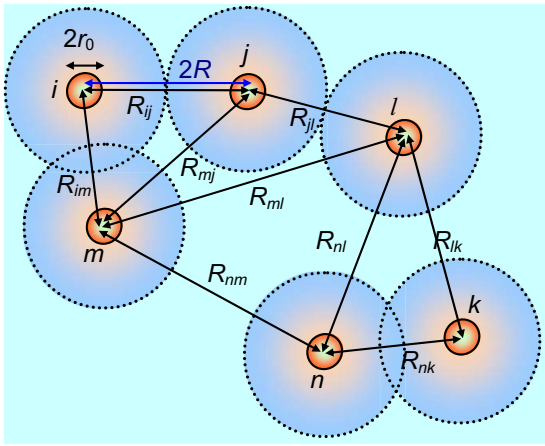

FIG. 1. Schematic presentation of spherical elastic defects with radius r_0 embedded into the matrix. The distance between defects "i" and "j" is R_{ij}. The average distance between defects is $2R$. The average volume per one defect is $V = \frac{4\pi}{3}R^3$.

In the general case, the structure of the Vegard expansion tensor W_{ij} [31–33] (elastic dipole) is controlled by the symmetry (crystalline or Curie group symmetry) of the material. In Eq. (4) the distance $r > r_0$. The elastic compliances tensor s_{ij} is written in Voight notations.

Substitution of elastic fields (4) into Eq. (2) leads to the renormalization of coefficient $\alpha(T) \to \alpha_{ij}^R$ by the joint action of electrostriction coupling and Vegard expansion,

$$\alpha_{kl}^R(T, \vec{r}) \approx \alpha(T) - 2Q_{ijkl}\sigma_{ij}^W(\mathbf{r}). \quad (5)$$

One can see from Eq. (5) that the local polar state occurred under the condition $\alpha_{kl}^R < 0$ is not excluded in the spatial regions, where the defect concentration is high enough. Let us make some estimates.

Using ergodic hypothesis, the averaging in Eq. (5) over the defect distribution function is reduced to the averaging over the defect partial volume, $V = \frac{4\pi}{3}R^3$, and gives the following expression:

$$\left\langle \alpha_{kl}^R(T, \bar{N}_d) \right\rangle \approx \alpha(T) - \frac{4}{3}Q_{ijkl}\tilde{W}_{ij}\bar{N}_d \ln\left(\frac{3}{4\pi\bar{N}_d r_0^3}\right), \quad (6a)$$

where $\tilde{W}_{ij} = c_{ijkl}W_{kl}$ and c_{ijkl} is the elastic stiffness tensor. A detailed derivation of Eq. (6) is listed in Appendix B of Ref. [17].

For a typical case, $\alpha(T) = \alpha_T(T - T_C^*)$, where T_C^* can be essentially smaller than room temperature or negative due to the relaxor component, such as 30% of PZN and disordering impurities 4% of La. Pure PZT (52/48) has a Curie temperature of about 393 °C. For a solid solution PZT (52/48), the coefficient $\alpha_T \approx 2.66 \times 10^5\,\mathrm{C^{-2}\,m\,J\,K^{-1}}$, electrostriction coefficients $Q_{11} = 0.0966\,\mathrm{m^4/C^2}$, $Q_{12} = -0.0460\,\mathrm{m^4/C^2}$, $Q_{44} = 0.08190\,\mathrm{m^4/C^2}$, and elastic stiffness $c_{11} = 1.696 \times 10^{+11}$ Pa, $c_{12} = 0.819 \times 10^{+11}$ Pa [34,35]. Vegard tensor is usually diagonal for oxygen vacancies in perovskites, but anisotropic, e.g., $W_{11} = 16.33\,\text{Å}^3$ and $W_{22} = W_{33} = -8.05\,\text{Å}^3$ for $SrTiO_3$ [33]. Note that the average concentration $\bar{N}_d$ should be much smaller than the value $2.25 \times 10^{28}\,\mathrm{m^{-3}}$ corresponding to one defect per unit cell with a size 4 Å.

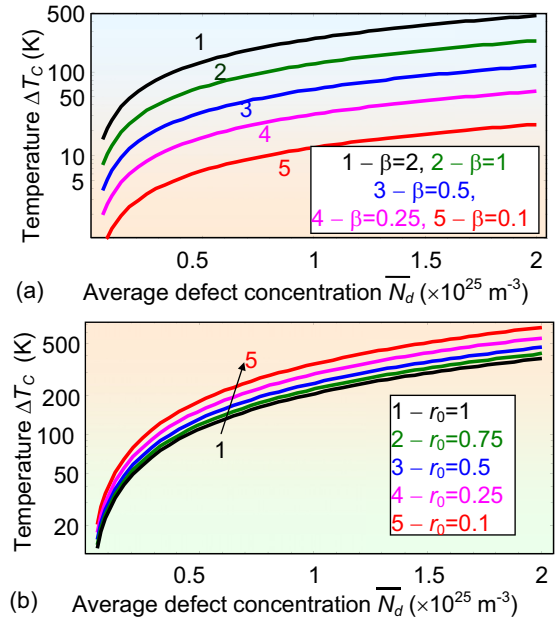

FIG. 2. (a) The shift of the Curie temperature ΔT_C vs the average concentration $\bar{N}_d$ of oxygen vacancies calculated for several values of the Vegard tensor amplitude $\beta = 2$ (curve 1), 0.5 (curve 2), 0.5 (curve 3), 0.25 (curve 4), and 0.1 (curve 5). Vegard strain tensor $w_{ii} = \beta W_{ii}$, where $W_{11} = 16.33\,\text{Å}^3$ and $W_{22} = W_{33} = -8.05\,\text{Å}^3$. Defect size is $r_0 = 0.5\,\text{Å}^3$. (b) The shift of the Curie temperature ΔT_C vs the average concentration of oxygen vacancies calculated for several values of the defect size $r_0 = 1$ (curve 1), 0.75 (curve 2), 0.5 (curve 3), 0.25 (curve 4), and $0.1\,\text{Å}^3$ (curve 5). Note that the dimensionless amplitude "beta" is introduced to demonstrate the influence of the Vegard stain on the properties.

Thus we obtain from expression (6a) that the renormalized transition temperature is equal to

$$T_C^R \approx T_C^* + \frac{4}{3\alpha_T}[Q_{11}\tilde{W}_{11} + Q_{12}(\tilde{W}_{22} + \tilde{W}_{33})] \times \bar{N}_d \ln\left(\frac{3}{4\pi\bar{N}_d r_0^3}\right). \quad (6b)$$

Here, T_C^* is an analog of the Curie temperature for a PZN relaxor, i.e., it originated from a soft mode, observed at $T = 20\,\mathrm{K}$ [21], and so T_C^* has to be negative and can be estimated as $T_C^* \approx -(5-100)\,\mathrm{K}$, similarly to estimations made from the soft mode observed in PMN [20]. Here, we introduced the Vegard stress tensor components as follows: $\tilde{W}_{11} = c_{11}W_{11} + c_{12}(W_{22} + W_{33})$, $\tilde{W}_{22} = c_{11}W_{22} + c_{12}(W_{11} + W_{33})$, and $\tilde{W}_{33} = c_{11}W_{33} + c_{12}(W_{11} + W_{22})$.

It follows from Eq. (6b) that the competition between contributions of the first and second terms can lead to $T_C^R > 0$ and so ferroelectricity could be observed. The shift of the Curie temperature ΔT_C versus the average concentration of oxygen vacancies $\bar{N}_d$ calculated for several values of the Vegard tensor amplitude and defect sizes are shown Figs. 2(a) and 2(b), respectively. The shift monotonically increases with increasing $\bar{N}_d$. Also, it increases with increasing Vegard coefficient and decreasing defect size. One can see from Fig. 2 that the polar phase is not excluded if the defect concentration

$\bar{N}_d$ is high enough. Keeping in mind that the oxygen vacancy concentration depends on technology [6], the special choice of $\bar{N}_d$ can overcome the correlation threshold necessary for the existence of a normal switchable ferroelectric phase.

It is noteworthy that the switchable ferroelectric polarization originates from the renormalization of Curie temperature given by Eq. (6b), and its two energetically equivalent (at zero external field) spontaneous values can be estimated as $P_{1,2} = \pm\sqrt{\frac{\alpha_T(T_C^K - T)}{\alpha_{11}}}$ in accordance with the mean-field approach. The values are the upper limit as estimated without gradient and depolarization effects, which decrease the polarization, and random fields, which can change it locally via disorder, as it will be analyzed in the next section. Note that it was shown earlier that Vegard strains and stresses coupled with electrostriction and flexoelectricity indeed can induce a reversible ferroelectric polarization in nanosized ferroelectrics, which are paraelectric otherwise [36,37].

It is important to underline that for intermediate concentration of oxygen vacancies the coexistence of a relaxor state and a ferroelectric phase can take place. It is not excluded that the result obtained by Deng *et al.* [6] for NS samples with $p = 1.53$ is characterizing neither ferroelectric nor relaxor phases and speaks in favor of the coexistence of different states, namely, of ordered ferroelectric and disordered relaxor states.

VI. LOCAL POLARIZATION AND ELECTRIC FIELD INDUCED BY FLEXO-CHEMICAL COUPLING IN A RELAXOR

Let us estimate the polarization and electric fields variations induced by the joint action of Vegard stresses and flexoelectric coupling. The equations of state $\partial G/\partial\sigma_{ij} = -u_{ij}$ give the strains u_{ij} as

$$u_{ij} = s_{ijkl}\sigma_{kl} + W_{ij}\delta N_d - F_{ijkl}\frac{\partial P_l}{\partial x_k} + Q_{ijkl}P_kP_l. \tag{7a}$$

Since the static equation of mechanical equilibrium, $\partial\sigma_{ij}/\partial x_j = 0$, should be valid, Eq. (7a) transforms into a Lame-type equation for elastic displacement U_i:

$$c_{ijkl}\frac{\partial^2 U_l}{\partial x_j\partial x_k} = \frac{\partial}{\partial x_j}\left(\sigma_{ij}^W - f_{ijkl}\frac{\partial P_l}{\partial x_k} + q_{ijkl}P_kP_l\right), \tag{7b}$$

where c_{ijkl} are the elastic stiffness, Vegard stress $\sigma_{mn}^W = c_{ijmn}W_{ij}\delta N_d$, $q_{mnkl} = c_{ijmn}Q_{ijkl}$ is the electrostriction stress tensor, and $f_{mnkl} = c_{ijmn}F_{ijkl}$ is the flexocoupling stress tensor.

Minimization of the Gibbs potential (2) with respect to P_j leads to the Landau-Ginzburg-Devonshire type equations for ferroelectric polarization components:

$$(\alpha\delta_{ij} - 2\sigma_{mn}Q_{mnij})P_j + \alpha_{ijkl}P_jP_kP_l - g_{ijkl}\frac{\partial^2 P_k}{\partial x_j\partial x_l} = F_{mnli}\frac{\partial\sigma_{mn}}{\partial x_l} + E_i. \tag{8}$$

The electric field E_i is the sum of internal (depolarizing and spatially random) and probing external fields, $E_i = \delta E_i + E_i^{\text{ext}}$, which should be found self-consistently from Eq. (3). Further, we put $E_i^{\text{ext}} = 0$ being interested in the random field only. For this case, Eq. (3) can be rewritten in the form of Poisson equation for an electric potential ϕ:

$$\varepsilon_b\varepsilon_0\frac{\partial^2\phi}{\partial x_i^2} = \frac{\partial P_i}{\partial x_i} + e(\delta N_d^+ - \delta n). \tag{9}$$

The conventional relation $E_i = -\partial\phi/\partial x_i$ is valid. Here ε_b is the background permittivity, which can be high enough $\sim(10^2{-}10^3)$ for relaxor ferroelectrics, for normal ferroelectrics it is no more than 10. The total electroneutrality condition $\bar{N}_d^+ = \bar{n}$ (valid at $E_i^{\text{ext}} = 0$) is already used in Eq. (9).

In Appendix A of Ref. [17], we solved the linearized system of Eqs. (7b), (8), and (9) using the method outlined in Ref. [38]. The Fourier **k** spectrum of the internal electric field variation (depolarizing by nature and random as it is induced by random variation of the defect concentration) was found in the Debye approximation from Eq. (9). It has the form

$$\delta\tilde{E}_j(\mathbf{k}) \approx \frac{-k_mk_j\delta\tilde{P}_m}{\varepsilon_b\varepsilon_0\left(k^2 + R_d^{-2}\right)}, \tag{10a}$$

where R_d is the screening radius that depends on the temperature and average concentration of defects as $R_d = \sqrt{\frac{\varepsilon_b\varepsilon_0k_BT}{2e^2\bar{N}_d}}$. The Fourier **k** spectrum of the polarization variation induced by the randomly distributed vacancies due to Vegard stresses and flexoelectric coupling has the following form:

$$\delta\tilde{P}_j(\mathbf{k}) \approx i\,f_{mnli}k_lk_nk_{j'}S_{mi'}(\mathbf{k})\tilde{\chi}_{ij}(\mathbf{k})\tilde{\sigma}_{i'j'}^W, \tag{10b}$$

Random stresses are related with the random vacancies sites as $\sigma_{mn}^W = c_{ijmn}W_{ij}\delta N_d$. The converse tensors of dielectric susceptibility $\tilde{\chi}_{ij}^{-1}(\mathbf{k})$ and elastic matrix $S_{ik}^{-1}(\mathbf{k})$ have the form

$$\tilde{\chi}_{ij}^{-1}(\mathbf{k}) \approx \alpha\delta_{ij} + g_{ipjl}k_pk_l + \frac{k_ik_j}{\varepsilon_b\varepsilon_0\left(k^2 + R_d^{-2}\right)},$$
$$S_{ik}^{-1}(\mathbf{k}) = c_{ijkl}k_lk_j, \tag{10c}$$

where c_{ijkl} are the elastic stiffness coefficients. The second term, $g_{ipjl}k_pk_l$, in the expression for $\tilde{\chi}_{ij}^{-1}(\mathbf{k})$ originates from the polarization gradient, and the third term, $\frac{k_ik_j}{\varepsilon_b\varepsilon_0(k^2+R_d^{-2})}$, originates from depolarization effects calculated in the Debye approximation. Also, it was shown earlier (see, e.g., Ref. [3]. and Refs. [14–16] therein) that the contribution of the gradient term is important for nanosized structures, while for homogeneous micrometer-sized structures, this contribution is negligible.

The variations of the random electric field (10a) and local polarization (10b) are not related with the ferroelectricity induced by uncharged vacancies with the average concentration $\bar{N}_d$ considered in the mean-field approach in Sec. V. The ferroelectric polarization is proportional to the nonzero average concentration of vacancies $\bar{N}_d$. The variation $\delta\vec{P}(\mathbf{r})$ is, of course, not switchable and its average value is zero, $\langle\delta\vec{P}(\mathbf{r})\rangle = 0$, since $\langle\delta N_d(\mathbf{r})\rangle = 0$.

That is why it makes sense to calculate standard (mean square) deviations of local polarization $\langle\delta\vec{P}^2(\mathbf{r})\rangle$ and electric field $\langle\delta\vec{E}^2(\mathbf{r})\rangle$, which are proportional to the dispersion of defect concentration $\langle\delta N_d^2(\mathbf{r})\rangle$. Note that analytical estimates of the values $\sqrt{\langle\delta\vec{P}^2(\mathbf{r})\rangle}$ and $\sqrt{\langle\delta\vec{E}^2(\mathbf{r})\rangle}$ are possible only for the case of

the simplest spherically symmetric dilatation center in an isotropic surrounding, while more realistically it is cubic. Analytical expressions for $\sqrt{\langle\delta\vec{P}^2(\mathbf{r})\rangle}$ and $\sqrt{\langle\delta\vec{E}^2(\mathbf{r})\rangle}$ are derived in Appendix A of Ref. [17], they are as follows:

$$\sqrt{\langle\delta\vec{P}^2(\mathbf{r})\rangle} \cong \frac{|f_{11}W_{\text{eff}}k_c|\sqrt{\langle\delta N_d^2\rangle}}{\left|\alpha_T(T-T_C^*)+g_{11}k_c^2+\frac{k_c^2R_d^2}{\varepsilon_b\varepsilon_0\left(1+k_c^2R_d^2\right)}\right|}, \tag{11a}$$

$$\sqrt{\langle\delta\vec{E}^2(\mathbf{r})\rangle} \cong \frac{k_c^2R_d^2|f_{11}W_{\text{eff}}k_c|\sqrt{\langle\delta N_d^2\rangle}}{\varepsilon_b\varepsilon_0\left(1+k_c^2R_d^2\right)\left|\alpha_T(T-T_C^*)+g_{11}k_c^2+\frac{k_c^2R_d^2}{\varepsilon_b\varepsilon_0\left(1+k_c^2R_d^2\right)}\right|}, \tag{11b}$$

where the effective Vegard coefficient $W_{\text{eff}} = W_{11}(1+2\frac{c_{12}}{c_{11}})$ and the wave vector $k_c \cong \xi\sqrt[3]{1/\bar{N}_d}$ characteristic for the long-range correlations are introduced. Since k_c defines the period of the long-range correlations, the dimensionless parameter ξ should be order of unity, and $k_c \ll \frac{1}{r_0}$ as anticipated.

Let us perform numerical estimates of the gradient term $(g_{11}k_c^2)$ and depolarization $[\frac{k_c^2R_d^2}{\varepsilon_b\varepsilon_0(1+k_c^2R_d^2)}]$ contributions in Eqs. (11) for typical values of parameters: gradient coefficient $g_{11} = (0.1-5)\times10^{-10}\,\text{m}^3/\text{F}$, inverse Curie-Weiss constant $\alpha_T \approx 2.66\times10^5\,\text{C}^{-2}\,m\,\text{J}\,\text{K}^{-1}$, virtual Curie temperature $T_C^* \approx -(5-100)\,\text{K}$, and relative permittivity $\varepsilon_b \sim 10^2$ for relaxor ferroelectrics. For chosen parameters, the "dressed" Debye screening radius R_d can be smaller than 0.8 nm at 293 K at $\bar{N}_d = 10^{25}\,\text{m}^{-3}$ and $\xi \sim 1$. For these values, the gradient and depolarization contributions are $g_{11}k_c^2 \sim \times10^5\,\text{C}^{-2}\,\text{m}\,\text{J}$ and $\frac{k_c^2R_d^2}{\varepsilon_b\varepsilon_0(1+k_c^2R_d^2)} \sim 0.8\times10^7\,\text{C}^{-2}\,\text{m}\,\text{J}$, respectively. These values are significantly smaller than the soft mode contribution $|\alpha_T(T-T_C^*)| \sim (0.81-1.06)\times10^8\,\text{C}^{-2}\,\text{m}\,\text{J}$ at room temperature. Since it is not excluded that for other parameters (e.g., for smaller ε_b and $\bar{N}_d$) the depolarization contribution can be compatible and even higher than the soft mode one, we note that Eqs. (10)–(11) are applicable for all parameters.

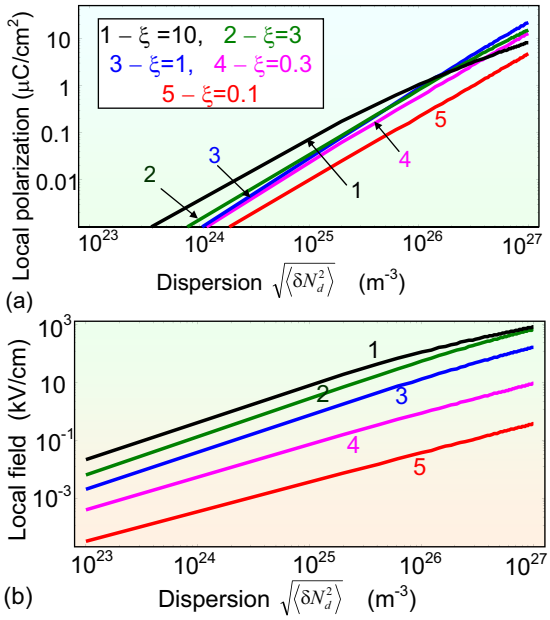

FIG. 3. Mean square deviations of (a) local polarization $\sqrt{\langle\delta\vec{P}^2(\mathbf{r})\rangle}$ and (b) electric field $\sqrt{\langle\delta\vec{E}^2(\mathbf{r})\rangle}$ vs the dispersion $\sqrt{\langle\delta N_d^2\rangle}$ of vacancy concentration fluctuations are shown in log-log scale for several values of parameter $\xi = 10$ (curve 1), 3 (curve 2), 1 (curve 3), 0.3 (curve 4), and 0.1 (curve 5). Vegard strain tensor strength $W = 10\,\text{Å}^3$ and flexocoupling constant $f_{11} = 4\,\text{V}$ estimated from Kogan model [44] and temperature $T = 300\,\text{K}$.

The dependencies of the mean square deviation of the local polarization, $\sqrt{\langle\delta\vec{P}^2(\mathbf{r})\rangle}$, and electric field, $\sqrt{\langle\delta\vec{E}^2(\mathbf{r})\rangle}$, on the dispersion $\sqrt{\langle\delta N_d^2\rangle}$ of the vacancy concentration fluctuations are shown in Figs. 3(a) and 3(b) for several values of dimensionless parameter ξ within the range $(0.1-10)$. The values $\sqrt{\langle\delta\vec{P}^2(\mathbf{r})\rangle}$ and $\sqrt{\langle\delta\vec{E}^2(\mathbf{r})\rangle}$ monotonically increase with increasing $\sqrt{\langle\delta N_d^2\rangle}$.

To resume the section, the dependence of the mean square deviation of polarization $\langle\delta P^2(\mathbf{r})\rangle$ and internal electric field $\langle\delta E^2(\mathbf{r})\rangle$ on the concentration of oxygen vacancies $\sqrt{\langle\delta N_d^2\rangle}$ [shown in Fig. 3] demonstrated that flexochemical coupling essentially contributes to local polarization and the internal electric field. This speaks in favor of the statement about existence of a dipole glass state. So that the proposed model explains and quantifies some features of the dipole glass and relaxor states coexistence [19], which has been observed experimentally [39–41].

VII. DISCUSSION AND CONCLUSIONS

The main experimental fact obtained in [6] originated from measurements of the temperature dependence of PZN-PLZT relaxor dielectric permittivity for NS and AO samples. The authors obtained respectively $p = 1.53$ and 1.91 in Eq. (1). These data speak in favor of the statement that in NS samples with large concentration of oxygen vacancies ferroelectricity is induced, so that we witness its coexistence with a relaxor state of PZN. The obtained result resembles a $PMN_{1-x}PT_x$ compound for which $p = 1.53$ can be obtained for $x = 0.5$ approximately. For this concentration, transition to the ferroelectric phase takes place at $T_C = 250\,^\circ\text{C} > 0$ in PMN-PT (see, e.g., [42]). The main task of our consideration was to find out the physical mechanism that can be responsible for the oxygen vacancy induced ferroelectricity in the PZN-PLZT relaxor. As a matter of fact, (Pb, La)$Zr_{0.52}Ti_{0.48}O_3$ with La content below 10% is known to be in a ferroelectric phase [43], which could suppress relaxor disorder of PZN. However, allowing for the value of parameter $p = 1.91$ for OA samples

annealed in oxygen is very close to $p = 2$, which is a characteristic value for relaxors, we neglected the PLZT contribution for NS samples, where $p = 1.53$ and the concentration of oxygen vacancies is large (see Introduction). Keeping in mind that oxygen vacancies are elastic dipoles, whose influence used to be considered as a Vegard mechanism, we performed the calculations with the help of a defect concentration distribution function and obtained Eq. (6). The results depicted in Fig. 2 show that at some average concentration of oxygen vacancies $\bar{N}_d$ their contribution can be larger than the negative value of temperature T_C^* of a relaxor and so we obtained a positive transition temperature, characteristic for a ferroelectric. For a transformation of a relaxor into a ferroelectric, one needs large enough concentration of oxygen vacancies and Vegard tensor amplitude. Unfortunately, the exact value of the negative Curie temperature T_C^* is not known and we have to discuss some estimation only. It is obvious that even a large enough value of T_C^* can be overcome by special choice of oxygen vacancy concentrations and other parameters. The latter is very important because the vacancy concentration has to be larger than the correlation threshold necessary for the existence of a normal ferroelectric reversible phase. In such a case at $T < T_C^R$ (ferroelectric phase), all the properties could be calculated with the conventional way on the basis of free energy $G = \frac{\alpha_T (T_C^R - T)}{2} P^2 + \frac{\alpha_{11}}{4} P^4$, so that, e.g., polarization $P^2 = \frac{\alpha_T (T_C^R - T)}{\alpha_{11}}$, while at $T > T_C^R$, the polarization is zero, $P = 0$, and we again have the relaxor. For this case in Sec. VI, we consider a local polarization and an electric field induced by the Vegard and flexoelectric effects (flexochemical coupling). The dependence of the mean square deviation of the polarization, $\langle \delta P^2(\mathbf{r}) \rangle$, and internal electric field, $\langle \delta E^2(\mathbf{r}) \rangle$, on the concentration of oxygen vacancies $\sqrt{\langle \delta N_d^2 \rangle}$ [shown in Fig. 3] speaks in favor of the existence of a dipole glass state. So that the proposed model can explain and quantify some features of the dipole glass and relaxor states coexistence, which has been observed experimentally [19,40–42].

Keeping in mind the accumulation of oxygen vacancies in the vicinity of different inhomogeneities, we came to the conclusion about oxygen vacancy concentration inhomogeneity. In such a case one can expect coexistence of a relaxor state and ferroelectricity. It is not excluded that this interesting phenomenon was observed by Deng [6] for NS samples with $p = 1.53$. It lays approximately at the same distance from $p = 2$ for relaxors and $p = 1$ for ferroelectrics. Therefore, at some concentration of oxygen vacancies and $T < T_C^R$, we are faced with a morphotrophic region in PZN-PLZT.

To resume, we have shown that the transition to a ferroelectric phase can be induced in a relaxor by the influence of oxygen vacancies being elastic dipoles due to the joint action of electrostrictive and Vegard couplings at some large enough concentration of the vacancies. In the regions where the concentration of vacancies is low, the local polarization and electric field could be induced by the flexochemical coupling in dependence on the concentration of oxygen vacancies. Because of the inhomogeneity of vacancy concentration, the coexistence of ferroelectricity and relaxor state can be expected.

ACKNOWLEDGMENTS

The authors express their deep gratitude to the Referees for very useful suggestions and comments.

M.D.G. generated the research idea, stated the problem, and wrote Secs. I–IV, discussion and conclusions of the manuscript. A.N.M. wrote Secs. V and VI and Appendix A of Supplementary materials with corresponding calculations and, jointly with E.A.E., generated figures. E.A.E., G.L., and S.V.K. worked on the results discussion and manuscript improvement. This work was supported by the US Department of Energy (DOE), Office of Science, Basic Energy Sciences (BES), Materials Sciences and Engineering Division (SVK).

[1] L. E. Cross, Ferroelectric materials for electromechanical transducer applications, Mater. Chem. Phys. **43**, 108 (1996).

[2] S.-E. Park and T. R. Shrout, Characteristics of relaxor-based piezoelectric single crystals for ultrasonic transducers, IEEE Transactions on Ultrasonics, Ferroelectrics, and Frequency Control **44**, 1140 (1997).

[3] M. D. Glinchuk, A. V. Ragulya, and V. A. Stephanovich, *Nanoferroics*, Springer Series in Materials Science (Springer, Dordrecht, 2013), p. 378.

[4] M. D. Glinchuk and R. Farhi, A random field theory based model for ferroelectric relaxors, J. Phys. Condens. Matter **8**, 6985 (1996).

[5] M. D.Glinchuk, Relaxor ferroelectrics: from Cross superparaelectric model to random field theory, Br. Ceram. Trans. **103**, 76 (2004).

[6] G. Deng, G. Li, A. Ding, and Q. Yin, Evidence for oxygen vacancy inducing spontaneous normal-relaxor transition in complex perovskite ferroelectrics, Appl. Phys. Lett. **87**, 192905 (2005).

[7] S. Steinsvik, R. Bugge, J. Gjonnes, J. Tafto, and T. Norby, The defect structure of $SrTi_{1-x}Fe_xO_{3-y}$(x = 0−0.8) investigated by Electrical Conductivity Measurements and Electron Energy Loss Spectroscopy (EELS), J. Phys. Chem. Solids **58**, 969 (1997).

[8] D. Woodward, I. M. Reaney, G. Y. Yang, E. C. Dickey, and C. A. Randall, Vacancy ordering in reduced barium titanate, Appl. Phys. Lett. **84**, 4650 (2004).

[9] N. Setter and L. E. Cross, The role of B-site cation disorder in diffuse phase transition behavior of perovskite ferroelectrics, J. Appl. Phys. **51**, 4356 (1980).

[10] C. Ang, Z. Yu, and L. E. Cross, Oxygen-vacancy-related low-frequency dielectric relaxation and electrical conduction in Bi: $SrTiO_3$, Phys. Rev. B **62**, 228 (2000).

[11] F. Wang, Z. Pang, L. Lin, S. Fang, Y. Dai, and S. Han, Magnetism in undoped MgO studied by density functional theory, Phys. Rev. B **80**, 144424 (2009).

[12] J. Carrasco, F. Illas, N. Lopez, E. A. Kotomin, Yu. F. Zhukovskii, R. A. Evarestov, Yu. A. Mastrikov, S. Piskunov,

and J. Maier, First-principles calculations of the atomic and electronic structure of F centers in the bulk and on the (001) surface of $SrTiO_3$, Phys. Rev. B **73**, 064106 (2006).

[13] H. Jin, Y. Dai, B. B. Huang, and M.-H. Whangbo, Ferromagnetism of undoped GaN mediated by through-bond spin polarization between nitrogen dangling bonds, Appl. Phys. Lett. **94**, 162505 (2009).

[14] In particular, density functional calculations show that the energy of vacancy formation on the surface is lower than in the bulk on about 3 eV for GaN [13] and 0.28 eV for MgO [11].

[15] C. Ziebert, H. Schmitt, J. K. Krüger, A. Sternberg, and K. H. Ehses, Grain-size-induced relaxor properties in nanocrystalline perovskite films, Phys. Rev. B **69**, 214106 (2004).

[16] H. Cao, F. Bai, J. Li, D. Viehland, G. Xu, H. Hiraka, and G. Shirane, Structural phase transformation and phase boundary/stability studies of field-cooled $Pb(Mg_{1/3}Nb_{2/3}O_3)$–32% $PbTiO_3$ crystals, J. Appl. Phys. **97**, 094101 (2005).

[17] See Supplemental Material at http://link.aps.org/supplemental/10.1103/PhysRevB.98.094102 for solution of linearized system of Euler-Lagrange equations and calculations of correlators.

[18] Erhart, Paul, and K. Albe, Dopants and dopant–vacancy complexes in tetragonal lead titanate: A systematic first principles study, Comput. Mater. Sci. **103**, 224 (2015).

[19] B. E. Vugmeister and M. D. Glinchuk, Dipole glass and ferroelectricity in random-site electric dipole systems, Rev. Mod. Phys. **62**, 993 (1990).

[20] P. M. Gehring, S. Wakimoto, Z.-G. Ye, and G. Shirane, Soft Mode Dynamics Above and Below the Burns Temperature in the Relaxor $Pb(Mg_{1/3}Nb_{2/3})O_3$, Phys. Rev. Lett. **87**, 277601 (2001).

[21] P. M. Gehring, S.-E. Park, and G. Shirane, Dynamical effects of the nanometer-sized polarized domains in $Pb(Zn_{1/3}Nb_{2/3})O_3$, Phys. Rev. B **63**, 224109 (2001).

[22] A. Kholkin, A. Morozovska, D. K. I. Bdikin, B. R. P. Wu, A. Bokov, Z.-G. Ye, B. Dkhil, L.-Q. Chen, and M. K. S. V. Kalinin, Surface domain structures and mesoscopic phase transition in relaxor ferroelectrics, Adv. Funct. Mater. **21**, 1977 (2011).

[23] R. Pirc, Z. Kutnjak, R. Blinc, and Q. M. Zhang, Electrocaloric effect in relaxor ferroelectrics, J. Appl. Phys. **110**, 074113 (2011).

[24] B. J. Rodriguez, S. Jesse, A. N. Morozovska, S. V. Svechnikov, D. A. Kiselev, A. L. Kholkin, A. A. Bokov, Z.-G. Ye, and S. V. Kalinin, Real space mapping of polarization dynamics and hysteresis loop formation in relaxor-ferroelectric $PbMg_{1/3}Nb_{2/3}O_3$−$PbTiO_3$ solid solutions, J. Appl. Phys. **108**, 042006 (2010).

[25] A. N. Morozovska, E. A. Eliseev, Y. A. Genenko, I. S. Vorotiahin, M. V. Silibin, Y. Cao, Y. Kim, M. D. Glinchuk, and S. V. Kalinin, Flexocoupling impact on the size effects of piezo- response and conductance in mixed-type ferroelectrics-semiconductors under applied pressure, Phys. Rev. B **94**, 174101 (2016).

[26] A. K. Tagantsev and G. Gerra, Interface-induced phenomena in polarization response of ferroelectric thin films, J. Appl. Phys. **100**, 051607 (2006).

[27] V. Westphal, W. Kleemann, and M. D. Glinchuk, Diffuse Phase Transitions and Random-Field-Induced Domain States of the "Relaxor" Ferroelectric $PbMg_{1/3}Nb_{2/3}O_3$, Phys. Rev. Lett. **68**, 847 (1992).

[28] Y. Imry and S.-k. Ma, Random-Field Instability of the Ordered State of Continuous Symmetry, Phys. Rev. Lett. **35**, 1399 (1975).

[29] B. I. Shklovskii and A. L. Efros, *Electronic Properties of Doped Semiconductors* (Springer-Verlag, Berlin, 1984).

[30] C. Teodosiu, *Elastic Models of Crystal Defects* (Springer-Verlag, Berlin, 1982).

[31] G. Catalan and J. F. Scott, Physics and applications of bismuth ferrite, Adv. Mater. **21**, 2463 (2009).

[32] X. Zhang, A. M. Sastry, and W. Shyy, Intercalation-induced stress and heat generation within single lithium-ion battery cathode particles, J. Electrochem. Soc. **155**, A542 (2008).

[33] D. A. Freedman, D. Roundy, and T. A. Arias, Elastic effects of vacancies in strontium titanate: Short-and long-range strain fields, elastic dipole tensors, and chemical strain, Phys. Rev. B **80**, 064108 (2009).

[34] M. J. Haun, E. Furman, S. J. Jang, H. A. McKinstry, and L. E. Cross, Thermodynamic theory of $PbTiO_3$, J. Appl. Phys. **62**, 3331 (1987).

[35] L.-Q. Chen, *Appendix A. Landau Free-Energy Coefficients*, in Physics of Ferroelectrics: A Modern Perspective, edited by K. Rabe, Ch.H. Ahn, and J.-M. Triscone (Springer-Verlag, Berlin, Heidelberg, 2007).

[36] A. N. Morozovska, I. S. Golovina, S. V. Lemishko, A. A. Andriiko, S. A. Khainakov, and E. A. Eliseev, Effect of Vegard strains on the extrinsic size effects in ferroelectric nanoparticles, Phys. Rev. B **90**, 214103 (2014).

[37] A. N. Morozovska and M. D. Glinchuk, Reentrant phase in nanoferroics induced by the flexoelectric and Vegard effects, J. Appl. Phys. **119**, 094109 (2016).

[38] A. N. Morozovska, Y. M. Vysochanskii, O. V. Varenyk, M. V. Silibin, S. V. Kalinin, and E. A. Eliseev, Flexocoupling impact on the generalized susceptibility and soft phonon modes in the ordered phase of ferroics, Phys. Rev. B **92**, 094308 (2015).

[39] Sh. M. Kogan, Piezoelectric effect during inhomogeneous deformation and acoustic scattering of carriers in crystals, Sov. Phys. Solid State **5**, 2069 (1964).

[40] V. V. Shvartsman, A. L. Kholkin, A. Orlova, D. Kiselev, A. A. Bogomolov, and A. Sternberg, Polar nanodomains and local ferroelectric phenomena in relaxor lead lanthanum zirconate titanate ceramics, Appl. Phys. Lett. **86**, 202907 (2005).

[41] V. V. Shvartsman, J. Dec, T. Łukasiewicz, A. L. Kholkin, and W. Kleemann, Evolution of the polar structure in relaxor ferroelectrics close to the Curie temperature studied by piezoresponse force microscopy, Ferroelectrics **373**, 77 (2008).

[42] W. Kleemann, V. V. Shvartsman, P. Borisov, and A. Kania, Coexistence of Antiferromagnetic and Spin Cluster Glass Order in the Magnetoelectric Relaxor Multiferroic $PbFe_{0.5}Nb_{0.5}O_3$, Phys. Rev. Lett. **105**, 257202 (2010).

[43] T. R. Shrout, Z. P. Chang, N. Kim, and S. Markgraf, Dielectric behavior of single crystals near the (1−X) $Pb(Mg_{1/3}Nb_{2/3})O_3$-(x) $PbTiO_3$ morphotropic phase boundary, Ferroelectrics Lett. Sec. **12**, 63 (1990).

[44] G. H. Haertling, PLZT electrooptic materials and applications—a review, Ferroelectrics **75**, 25 (1987).